Charge separation and recombination in radial ZnO/In$_2$S$_3$/CuSCN heterojunction structures

J. Tornow[1], K. Schwarzburg[2] *, A. Belaidi[2], T. Dittrich[2], M. Kunst[2], T. Hannappel[2]

[1] Fritz Haber Institute of the Max Planck Society, Department of Inorganic Chemistry, Faradayweg 4−6, Berlin, Germany

[2] Helmholtz Zentrum Berlin, Hahn-Meitner-Platz 1, 14109 Berlin, Germany

* Corresponding author: e-mail schwarzburg@helmholtz-berlin.de,

Abstract

A ZnO-nanorod/In$_2$S$_3$/CuSCN radial hetero structure has recently shown promising photovoltaic conversion efficiencies. In this work, the charge separation and recombination in single ZnO/ In$_2$S$_3$ and In$_2$S$_3$/CuSCN interfaces as well as the complete ZnO/In$_2$S$_3$/CuSCN structure were studied by time resolved microwave photoconductivity. Photoconductivity transients were measured for different thicknesses of the In$_2$S$_3$ light absorbing layer, under variation of the exciting light flux and before and after annealing of the ZnO nanorods at 450°C. Upon excitation with 532nm light, a long lived (ms) charge separation at the In$_2$S$_3$/ZnO interface was found, whereas no charge separation was present at the In$_2$S$_3$/CuSCN interface. The presence of the CuSCN hole conductor increased the initial amplitude of the TRMC signal of the In$_2$S$_3$/ZnO interface by a factor of 8 for a 6nm thick In$_2$S$_3$ layer, but the enhancement in amplitude dropped strongly for thicker films. The measurements show that the primary charge separation is located at the In$_2$S$_3$/ZnO interface but the charge injection yield into ZnO depends critically on the presence of CuSCN.

1. Introduction

The combination of different nanoscale materials into one composite macroscopic material opens a wide area of novel applications. Within the field of photovoltaics several such composite materials are currently under development. The prototype for this new class is certainly Grätzel's dye sensitized solar cell (1) where organic dyes and anorganic nanoparticles form a 3D assembly of charge separating heterostructures. The bulk heterojunction organic solar cell (2) follows the same idea using polymers as a light absorber. Even in recent silicon solar cell concepts heterostructures on a sub micron scale play a role, such as in microcrystalline Si having a 3D internal interface to amorphous Si. In the composite materials mentioned, the morphology of the microstructure has been found to be one of the key issues but it is generally hard to control. By starting with one material that already templates an appropriate structure, this problem can be overcome. Currently, arrays of vertical nano wires, rods or tubes seem to be the most promising candidate for this task (3-7). For low cost solar cell designs, ZnO nanorod arrays that can be grown at low temperatures by either chemical bath deposition (8) or electrodeposition are particularly promising (7). Recently, we have shown 3.4% conversion efficiency for a nanorod ZnO/In$_2$S$_3$/CuSCN solar cell (9). In theory, with a surface enhancement by a factor of 10 (roughness factor) efficiencies of about 10%–15% can reasonably be achieved with an absorber thickness of only about 20–30 nm (10).

The nanorod ZnO/In$_2$S$_3$/CuSCN solar cell consists of arrays of ZnO nanorods grown on a conductive glass substrate with a thin (<50nm) conformal layer of In$_2$S$_3$ on top that acts as the light absorber. This structure is filled with the p-conducting CuSCN by impregnation, before the final metalization is applied. In previous work, the photovoltaic properties of this solar cell as a function of the nanorod length (11), In$_2$S$_3$ absorber thickness (9) and sample annealing (12) were studied. In particular it was found that the In$_2$S$_3$ thickness plays a crucial role for the cell performance. Although the light absorption could be increased

Charge separation and Recombination in radial ZnO/In$_2$S$_3$/CuSCN heterojunction structures, J. Tornow et al..,
J. Appl. Phys. 108 (2010) 044915

2

with increasing In$_2$S$_3$ thickness, a drastic drop in the short circuit current was observed for thicker films (9). For very thin films (<10nm) a strong reduction of the open circuit voltage Voc was found. For an optimum cell efficiency, a thickness on the order of 20nm was required. The details of the charge separation and recombination processes involved are not well known. To further improve the cell efficiency, the processes that are limiting need to better understood. Time resolved microwave conductivity (TRMC) is an excellent tool for probing charge carrier dynamics without the need for electrical contacts (13). In this work we have employed the TRMC method to study the photo generation of charges and their recombination dynamics for the ZnO/ In$_2$S$_3$ and the In$_2$S$_3$/CuSCN hetero structure separately as well as for the full ZnO/In$_2$S$_3$/CuSCN hetero structure as used in the solar cell. Since TRMC is a contactless method we could grow the hetero structures directly on glass without a conducting layer (SnO2:F) underneath. The latter is required for obvious reasons in the solar cell, but might introduce additional recombination effects that are better studied separately.

Figure 1: SEM images of In$_2$S$_3$ covered ZnO nanorods after 8 (a), 15 (b), 30 (c) and 45 (d) ILGAR spray cycles. In the inset the coated rods mean diameter is plotted versus the number of spray cycles.

2. Experimental

Arrays of ZnO nanorods were prepared by chemical bath deposition on a glass substrate, which was coated with a 50nm thick sputtered ZnO seed layer. The aqueous growth solution contained 10 mmol/l zinc nitrate hexahydrate (Merck, ≥ 99% purity) and 0.4 mol/l sodium hydroxide (Merck, ≥ 99% purity) and was heated to 80°C for nanorod growth. A thorough investigation of the ZnO nanorod preparation by this solution method is given by Peterson et al. (8). The substrates were immersed into the solution at 80°C and left inside for 50 min. Afterwards the samples were successively rinsed with deionized water and pure ethanol. A post annealing step at 450°C for 1h in air was performed for some samples as indicated in the text.

A radial ZnO / In$_2$S$_3$ heterojunction was prepared by covering the nanorods with indium sulfide (In$_2$S$_3$) using the Spray-ILGAR process described in (14). An ethanolic solution of 25 mmol/l indium chloride (Alfa Aesar, 99.99%) was sprayed for 30 sec. at 200°C with a nitrogen carrier gas. After 10 sec of nitrogen purging the samples were exposed to hydrogen sulfide gas (95% Ar, 5% H$_2$S) for 14 sec succeeded by another 10 sec of nitrogen purging. This preparation cycle was repeated several times to achieve the desired In$_2$S$_3$ layer thickness. In Fig. 1 the SEM images of In$_2$S$_3$ covered ZnO nanorods for different Spray ILGAR cycles are shown. The thickness of the In$_2$S$_3$ layer was determined by measuring the diameter D of the In$_2$S$_3$ covered ZnO nanorods from the SEM images and plotting it versus the number of spray cycles. Fig. 1 shows a linear dependency and the In$_2$S$_3$ layer thickness equals $(D-D_0)/2$. D_0 is the diameter of the blank ZnO nanorod, given by the intersection of the linear fit with the abscissa in Fig. 1.
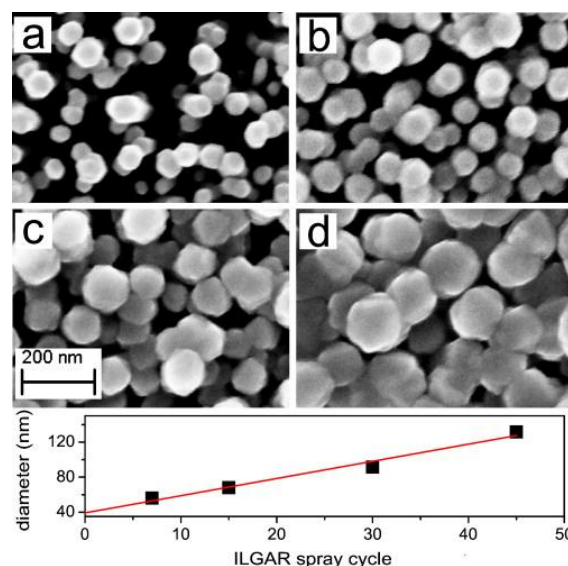
For the formation of a ZnO / In$_2$S$_3$ / CuSCN heterojuncion a saturated solution of CuSCN (Aldrich, 99%) and propyl-sulfid (Aldrich, 97%) was mixed and deposited onto the In$_2$S$_3$ covered ZnO nanorods by impregnation [7].

Optical transmission T of In$_2$S$_3$ covered ZnO nanorods was measured with a Perkin Elmer Lambda 35 UV-Vis spectrometer equipped with an integrating sphere. The absorption 1-T increased roughly linear with the In$_2$S$_3$ layer thickness and the intersection with the abscissa was used to estimate the transmission T_0 of the ZnO nanorods. From this the absorption of In$_2$S$_3$ was calculated through $1-(T-T_0)$.

Time resolved microwave conductivity (TRMC) (13, 15) is a contactless measurement where the change in the conductivity $\Delta\sigma(t)$ of a sample introduced by an optical excitation with a short laser pulse is monitored versus time. The sample is placed at one end of a GHz cavity and the change in microwave power $(\Delta P(t)/P)$ is recorded. For small perturbations of the conductivity, the change in microwave power is proportional to the change in conductivity (13).

$$\frac{\Delta P(t)}{P} = A \cdot \sigma(t) \qquad (1)$$

The sensitivity factor A is characteristic to the setup. A microwave frequency of 30 GHz was used. The samples were exited at 355 or 532 nm with a Nd:YAG laser having a 3mm spot size. The pulse width was 10 ns FWHM and the photon flux per pulse was adjusted by neutral density filters from 15 μJ/cm^2 (4x10^{13} cm^{-2}) to 15 mJ/cm^2 (4x10^{16} cm^{-2}). The transients were recorded by a Tektronix TDS 7154B digital oscilloscope and amplified through a 500

Charge separation and Recombination in radial ZnO/In$_2$S$_3$/CuSCN heterojunction structures, J. Tornow et al..,
J. Appl. Phys. 108 (2010) 044915

3

MHz , 60 dB gain AC-amplifier with a lower cut off frequency of 500Hz.

Generally, in a heterogeneous material structure the TRMC signal (eq.1) reflects the sum of all excess conductivities in each layer. Since the CuSCN/In$_2$S$_3$/ZnO hetero structure studied in this work is supposed to separate charges we can expect not only the number of excess charges to change over time but also the mobility of this charges might change. We can then write the total conductivity in eq.1 as the sum of electron and hole conductivities in each layer:

$$\sigma(t) = e \sum_i \mu_i^n n_i(t) + \mu_i^p p_i(t) \qquad (2)$$

where the summation is over the electron and hole conductivities in each layer.

3. Results

Fig.2 shows the transient microwave conductivity signals for a 180nm thick planar layer of In$_2$S$_3$ on glass and a 10nm thick In$_2$S$_3$-layer on ZnO nanorods. The thickness of the planar In$_2$S$_3$ film was chosen to give roughly the same optical absorption as the coated nanorod film and both transients were recorded under identical excitation conditions (533nm). The dashed curve shows the response of a plain ZnO nanorod electrode upon bandbgap excitation with 355nm light for comparison. The planar In$_2$S$_3$-layer gives a signal that is more than 10 times smaller in amplitude than the In$_2$S$_3$ coated nanorod sample. Furthermore the planar sample showed a time response that is comparable to the exciting laser pulse. Hence the lifetime of the excess carriers in the In$_2$S$_3$ film is equal or shorter than 10ns. Considering the mediocre material quality (low temperature processing) and the high interface ratio we actually expect the lifetime to be much shorter than this, more likely in the range of 10-100ps. The dramatic increase in both signal amplitude and TRMC decay time when the hetero contact is formed between the In$_2$S$_3$ absorber and the ZnO nanorod must be due to charge separation at at the interface. Only the spatial separation of electrons and holes is able to enhance their apparent lifetime from the sub ns range to the us-ms range (16). There is no indication of a delayed rise time in the In$_2$S$_3$/ZnO sample and thus the time scale of the charge separation process is well below the duration of the laser pulse. This indicates that we are only sensitive to the charge separated state: the TRMC signal is proportional to the sum of excess conductivities caused by electrons in the ZnO and holes in the In$_2$S$_3$ phase. If the carrier mobilities are considerably different, the one with the higher mobility will dominate the signal. Since the lifetime in the plain In$_2$S$_3$ reference sample is shorter than the time resolution of the experiment, it is not possible to estimate the In$_2$S$_3$ carrier mobility from the signal amplitude. The much smaller signal could be either caused by a very short lifetime, a low
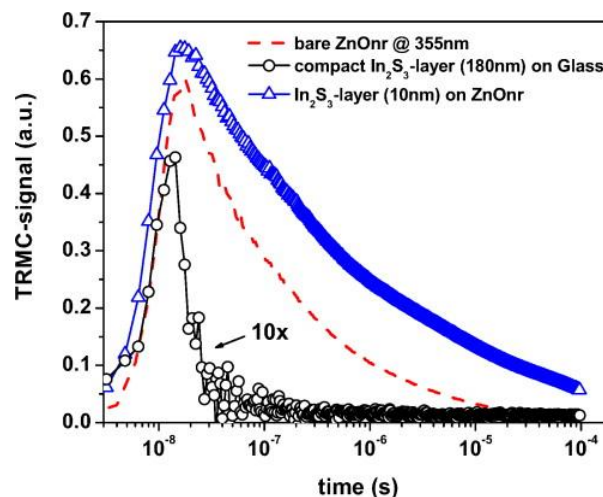

Figure 2: TRMC signal of a planar In$_2$S$_3$ layer and In$_2$S$_3$ covered annealed ZnO nanorods, exited with 532 nm at a photon flux of 4×10^{16} cm^{-2}. The TRMC signal of an annealed bare ZnO nanorod sample, excited with 355nm at a photon flux of 9×10^{13} cm^{-2} is plotted for comparison.
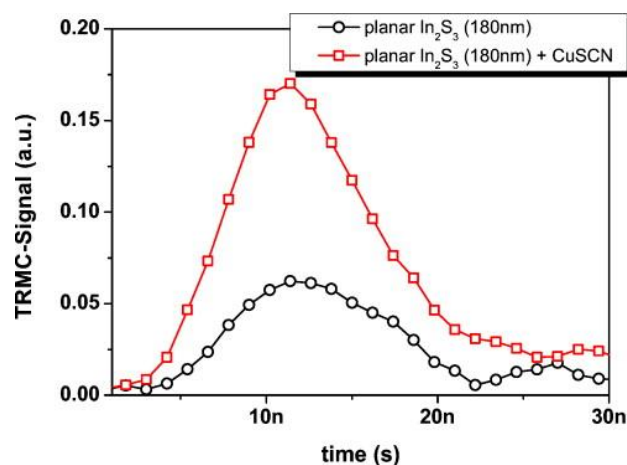

Figure 3: TRMC signal of a planar In$_2$S$_3$ layer on glass with and without CuSCN on top. Photon flux was 8×10^{16} cm^{-2}.

mobility or a mixture of both. However, by comparing the amplitude measured in ZnO at 355nm excitation (Fig.2 red dashed curve) and Dye sensitized ZnO (not shown) which are about the same for a similar excitation level, we conclude that the signal observed in In$_2$S$_3$/ZnO samples is mostly due to electrons in the ZnO. Note that the decay for both ZnO and In$_2$S$_3$/ZnO cannot be described by a single exponential time constant. In summary the measurement proves that a strong charge separation takes place at the In$_2$S$_3$/ZnO interface.

The second relevant hetero interface in the solar cell is the CuSCN/ In$_2$S$_3$ interface. To test whether this interface does also play a role in the charge separation process, a planar CuSCN/ In$_2$S$_3$ interface was prepared on a glass substrate. The lower curve (circles) in fig.3 belongs to the microwave conductivity of the In$_2$S$_3$ film alone and the curve with the square symbols was measured after deposi
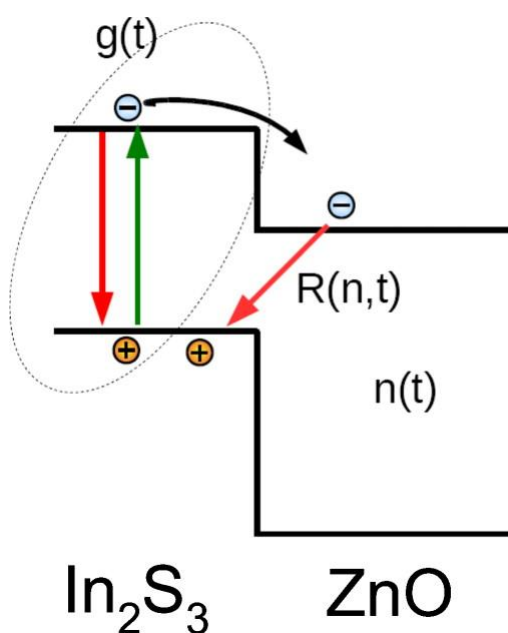
Charge separation and Recombination in radial ZnO/In$_2$S$_3$/CuSCN heterojunction structures, J. Tornow et al..,
J. Appl. Phys. 108 (2010) 044915

4

Figure 4: Illustration of the carrier dynamics in the presence of ZnO observed in the TRMC measurement.

Figure 5: Light absorption of the In$_2$S$_3$ layer on ZnO nanorods (a) and the corresponding TRMC amplitude of the In$_2$S$_3$ covered ZnO nanorods (b) as a function of the In$_2$S$_3$ layer thickness at a photon flux of 8×10^{14} cm^{-2}.

tion of CuSCN. Signal amplitudes were very low for the high excitation photon density of 8×10^{16} photons/cm^2 and the signal followed approximately the shape of the excitation pulse. The peak photoconductivity in fig.3 increased by a factor of 2.5 with the addition of the CuSCN layer. The reason for this can be either a passivation effect that increases the lifetime or a change in mobility when the holes enter the CuSCN phase. Relatively high hole mobilities of around 10cm^2/(Vs) were reported for CuSCN (17). In principle it is thus possible that the microwave signal becomes sensitive to holes entering the CuSCN layer.

Summarizing the previous findings, fig. 4 shows a sketch of the major dynamic processes that determine the TRMC response in our samples. First, there is electron hole pair generation in the In$_2$S$_3$ layer by the exciting laser pulse. Carrier transport within the In$_2$S$_3$ layer and charge separation at the interface are not time resolved. Hence we can lump all these processes into a single generation term g(t) for the injection rate of electrons into the ZnO electrode. The injection rate determines the peak amplitude of the TRMC signal. The decay of the TRMC signal is caused by the decrease of excess charges via electron hole recombination at the interface with a rate R x n(t). The recombination rate R is a function of the spatial overlap between electrons and holes and thus in general changes with time. Since we are only sensing the charge separated state, the TRMC signal refers to the same excess charge carriers as a photovoltage signal.

Figure 5 shows the light absorption (Fig.5a) of the In$_2$S$_3$ coated electrodes and the TRMC amplitude (Fig. 5b) as a function of the In$_2$S$_3$ thickness. The light absorption increases roughly linear with the In$_2$S$_3$-layer thickness and is not influenced by the ZnO annealing step at 450C. The TRMC amplitude of the annealed sample (Fig. 5b) simply
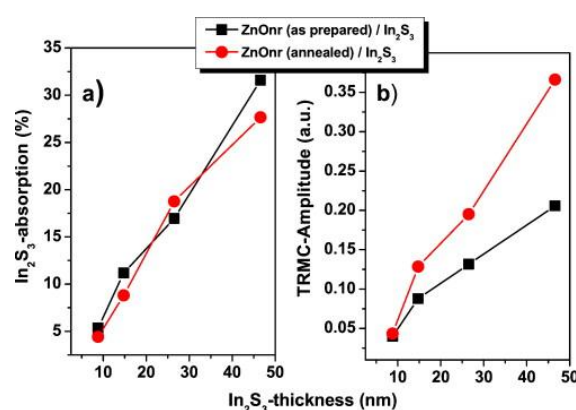
increased according to the increase in absorption. This demonstrates that even for the thickest absorbers used (45nm), the injection yield is not yet diminished by the finite excess carrier lifetime in the In$_2$S$_3$ layer. Correspondingly, the diffusion length is at least on the order of the film thickness (45nm). The TRMC amplitudes of the as prepared samples were consistently lower and showed some degradation with increasing In$_2$S$_3$ thickness. In contrast, we found that the TRMC amplitudes for band to band excitation at 355nm of bare ZnO nanorods were much less sensitive to the annealing. This suggests that the reduced amplitudes of the as prepared samples (Fig. 5b) have a different origin than ZnO electron mobility changes caused by the annealing. Since both annealed and non annealed nanorods were coated during the same run, an effect of variations in the In$_2$S$_3$ preparation can be excluded. If we assume that the In$_2$S$_3$ layer grown on the as prepared ZnO has similar electronic properties as the ones grown on the annealed samples, the apparent reduction in amplitude must be related to a reduction in charge separation efficiency, e.g. the electronic properties of the ZnO / In$_2$S$_3$ interface such as band alignment and interface states. It must be remarked that the measured absorption values are rather low compared to the absorption properties of a complete solar cell (9) where even the external quantum efficiency at a wavelength of 532nm exceeded 60% for an In$_2$S$_3$ thickness of about 25 nm. The reason for this is 2-fold: ZnO nanorods on glass substrate as used in this work grow almost perfectly perpendicular to the substrate surface whereas ZnO nanorods on FTO substrate, as used in complete solar cells, are randomly tilted which improves light harvesting. Secondly, the final low temperature annealing step used in the solar cell preparation causes Cu diffusion from the CuSCN hole conductor into the In$_2$S$_3$ layer that gives rise to a significant decrease in the bandgap and increased absorption at 532nm (12).

Fig. 6 shows the correlation between the TRMC amplitude and the intensity of the exciting laser pulse. A linear dependency of the TRMC amplitude is only observed for
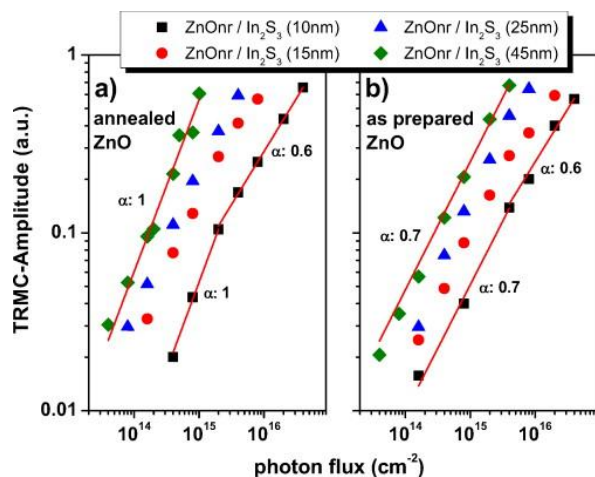
Charge separation and Recombination in radial ZnO/In₂S₃/CuSCN heterojunction structures, J. Tornow et al..,
J. Appl. Phys. 108 (2010) 044915

5

Figure 6: TRMC amplitude of In_2S_3 covered annealed (a) and non annealed (b) ZnO nanorods for different In_2S_3 layer thicknesses as a function of the exciting light flux.

moderate laser excitation intensities and only for the annealed sample (Fig.6a). The straight lines in Fig.6 are fits to the TRMC peak data (A_{TRMC}) by the following equation:

$$A_{TRMC} = n \cdot I^\alpha \qquad (3)$$

The laser intensity I is given as photons per pulse per area (in cm²) (n and α are fit constants). For an equivalent of a planar 200nm thick In_2S_3 layer with an absorption in the range of 20%, the total excess carrier concentration generated by one laser pulse at a photon density of $10^{15}cm^{-2}$ is about $10^{18}cm^{-3}$. It should be noted that this total excess carrier concentration is only the time integral of the laser pulse. Because of the fast charge separation and recombination dynamics that take place on a time scale shorter than the pulse duration, the transient concentration of excess charges in the In_2S_3 layer at each time t is significantly lower. Since with all samples we are far from complete light absorption, the excess carrier density in the In_2S_3 absorber should be roughly the same for a given photon density. For the annealed samples, the non-linear regime (α<1) is found at photon densities above $10^{15}cm^{-2}$. The finding that the appearance of the nonlinear regime is related to the excess charges generated in the In_2S_3 layer and not the total amount of separated charges (TRMC amplitude) indicates that the nonlinear process can be attributed mostly to the recombination process within the In_2S_3. Most likely, at this excess carrier concentration the high injection regime with bimolecular recombination is entered. However, the extreme heterogeneity of the present system prevents a quantitative description of this process but it can be expected that the bimolecular regime starts at excess carrier concentrations on the order of the majority carrier concentration. In the present case charge separation competes with band to band recombination on a ps timescale and thus it is impossible to relate the observed threshold intensity to a ma-

jority carrier density without a detailed knowledge of the relevant rate constants.

Within the sensitivity limits of our measurement we were not able to observe a linear intensity regime for the as prepared samples (Fig. 6b). Typical exponential factors of 0.7 were found even at the lowest intensities. This could also be due to a slower charge separation as discussed before. For example, if some kind of electronic barrier at the interface causes the electrons to remain for a longer time inside the In_2S_3 layer, the chance for a direct recombination rises. The dependency of the solar cells short circuit current on light intensity is characterized by a power law with an exponent of 0.85 for both annealed and as prepared nanorods (12). In the simplest case one would expect the same dependency on light intensity for both the short circuit photocurrent and the TRMC amplitude. The differences to the present results may be related to recombination at the substrate, the presence of CuSCN and the lower light intensity used in the stationary measurements.

So far we have mainly discussed the changes in amplitude of the TRMC signals and that a linear regime was observed at the lower intensities, at least for the annealed samples (fig.6). In fig.7 the microwave decay of the 10nm In_2S_3 sample is shown for different excitation levels. All curves were normalized to a peak amplitude of 1. The decay becomes noticeably faster with increasing light intensity and cannot be well described by single or double exponential terms. This nonlinear recombination behavior is not too surprising if we consider how much the hetero interface is charged in this experiment. At a photon density of 10^{14} photons/cm² and and a quantum efficiency of 10%, we generate a photocharge of 1.6uC/cm². Taking the typical capacitance of the ZnO nanorod electrode of about 5uF/cm² (18), an initial photovoltage of 300mV is generated even at a rather low intensity. At higher intensities the equilibrium space charge field becomes compensated by the transient charges and electrons are no longer withdrawn from the In_2S_3/ZnO interface. Regardless of the details involved, the
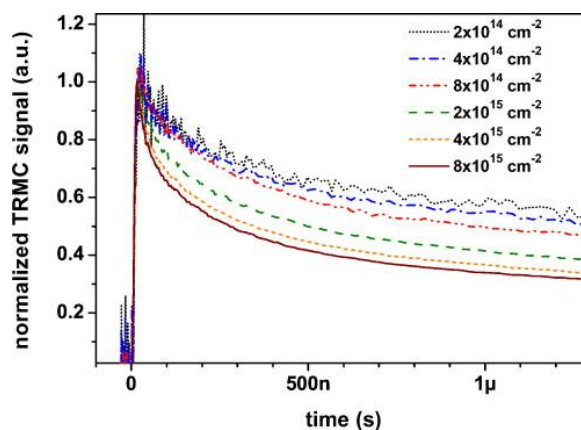

Figure 7: TRMC decay of a 10nm In_2S_3 /ZnO sample as a function of the light flux.

Charge separation and Recombination in radial ZnO/In$_2$S$_3$/CuSCN heterojunction structures, J. Tornow et al..,
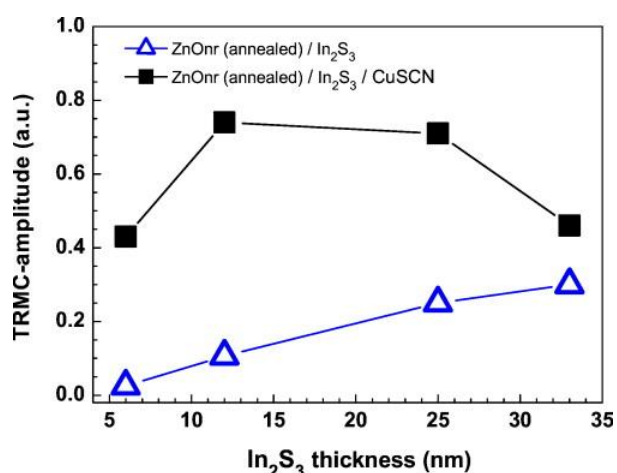J. Appl. Phys. 108 (2010) 044915

6

Figure 8: TRMC amplitude of In$_2$S$_3$ covered annealed ZnO nano-rods with and without CuSCN contact. TRMC amplitudes were measured for different thicknesses of the In$_2$S$_3$ layer at a photon flux 8×10^{14} cm^{-2}.

Figure 9: Normalized TRMC decay of the ZnO/In$_2$S$_3$/CuSCN hetero structure for a 6 and 12nm thick In$_2$S$_3$ layer. The 6nm In$_2$S$_3$ sample without CuSCN is shown for reference. The photon flux was 8×10^{14} cm^{-2}.

charging of the electrode increases the spatial overlap between electrons and holes and thus facilitates recombination. Even without a precise model for the decay we can take it as a fingerprint for the recombination rate of different samples, as long as the injection level is the same. By the nature of the recombination process, the data is relevant for the operation of the solar cell under load (fill factor and open circuit voltage) and not the short circuit condition.

Impregnation of p-conducting CuSCN into the In$_2$S$_3$ covered ZnO nanorods resulted in a strong increase of the TRMC amplitude as shown in figure 8. Especially for thin In$_2$S$_3$-layers the TRMC amplitude increases significantly up to a factor of eight. With thicker In$_2$S$_3$-layers the amplitude is still higher than for a system without CuSCN, but the differences become smaller. With increasing absorber thickness also the voids between adjacent nanorods become smaller (see fig.1). Thus we likely see the same kind of limitation with respect to incomplete CuSCN penetration we have noticed before in the solar cell preparation (9). Also compare the increase in amplitude shown in fig.3 for the planar In$_2$S$_3$ film (without the ZnO). The result that in the thick planar In$_2$S$_3$ film the signal is raised by a factor of 2.5 while for the 45nm layer on the nanorod structure the factor is only 1.4, further supports the assumption of a poor CuSCN penetration. Another explication lies in the poor charge separation of the CuSCN/ In$_2$S$_3$ interface (cf fig.3 and its explication): the experiments suggest that charge injection at the CuSCN/ In$_2$S$_3$ interface becomes effective in the presence of charge separation at the ZnO/ In$_2$S$_3$ interface.

In a previous paper it was shown that the fill factor and open circuit voltage of the solar cell dropped dramatically for very thin (<10nm) In$_2$S$_3$ layers (9). Fig.9 shows how the recombination characteristics seen in the photoconductivity are altered for very thin In$_2$S$_3$ layers if CuSCN is added. There is a strong reduction in decay time for the 6nm thick In$_2$S$_3$ layer if we bring it in contact with CuSCN.

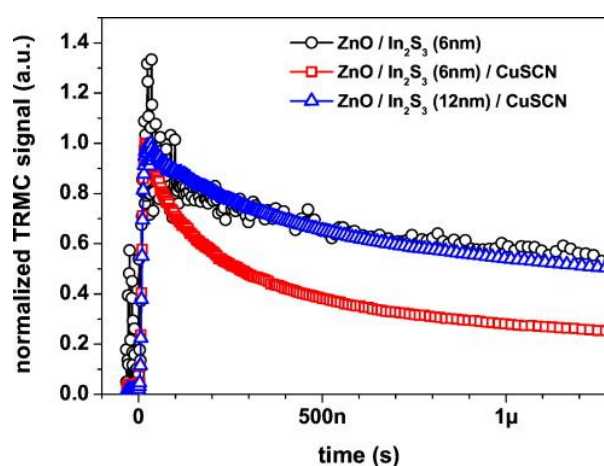By increasing the In$_2$S$_3$ thickness to 12nm, the slower decay characteristics of the CuSCN free sample is almost recovered. Hence, despite the fact that the CuSCN increases the TRMC amplitude, it has a negative effect on the recombination rate. The faster recombination are likely caused by a combination of a direct short circuit between CuSCN and ZnO through pinholes and increased tunneling trough the In$_2$S$_3$ layer. If we compare the results with that of the solar cell, it is clear that the poor cell results for very thin In$_2$S$_3$ layers are only related to the CuSCN being more closer to the ZnO interface and not to problems with the very thin layers itself. The result also shows that the poor solar cell performance is not exclusively related to a short circuit problem at the conducting glass substrate (SnO$_2$). The samples used in this work for the TRMC experiment were grown on a regular glass substrate without a conductive SnO$_2$ layer.

4. Discussion

Based on our previous work (9, 12, 11), the purpose of this investigation was to clarify the charge separation process and to gain a better understanding of the limiting factors in the ZnO nanorod / In$_2$S$_3$ / CuSCN solar cell. The first important result is the long lived charge separation at the In$_2$S$_3$ / ZnO interface (fig.2). In contrast, the In$_2$S$_3$ / CuSCN interface alone did not give evidence for an efficient long lived charge separation. We found that for ZnO/In$_2$S$_3$ samples without CuSCN the amplitude scaled roughly linear with the optical absorption of the In$_2$S$_3$ layer (fig5). This result suggests that diffusion length of the photoexcited state in In$_2$S$_3$ is at least on the order of 30nm. Adding CuSCN increased the amplitude very strongly for the thinnest In$_2$S$_3$ layers but had a lesser effect for thicker In$_2$S$_3$ layers (fig.8). Although there was a further increase in light absorption, the TRMC amplitude of the CuSCN

Charge separation and Recombination in radial ZnO/In$_2$S$_3$/CuSCN heterojunction structures, J. Tornow et al..,
J. Appl. Phys. 108 (2010) 044915

7

samples was saturated already at a thickness around 10nm and did decrease above 30nm. The quantum yield for the charge separation is proportional to the TRMC amplitude divided by the number of absorbed photons. In the presence of CuSCN the quantum yield thus drops for In$_2$S$_3$ layers thicker than 10nm. A similar trend was observed in the short circuit current of the solar cells, which was found highest for the thinnest In$_2$S$_3$ layers and decreased strongly for thicker layers (9). Obviously CuSCN is needed in close proximity to the ZnO nanorods for an efficient charge separation and there seems to be a principal difference between the charge separating process in the ZnO/In$_2$S$_3$ and the ZnO/In$_2$S$_3$ /CuSCN hetero structure. Two major factors may account for the differences: passivation of the In$_2$S$_3$ surface by CuSCN and differences in the dark equilibrium charge and potential distribution. In addition we also need consider the effect of Cu diffusion into In$_2$S$_3$. Passivation of the In$_2$S$_3$ surface by CuSCN against recombination alone cannot explain the data. Firstly, if recombination at the In$_2$S$_3$ /air interface would dominate the excess carrier lifetime in the In$_2$S$_3$ absorber of the ZnO/In$_2$S$_3$ structure, an increase in the layer thickness should reduce the influence of the interface and the effective lifetime should increase. This in turn would increase the quantum yield for charge injection into ZnO. Hence the increase in TRMC amplitude with the In$_2$S$_3$ layer thickness should be stronger than observed. Secondly, a reduction in interface recombination cannot explain the drop in charge injection for the thicker In$_2$S$_3$ layers in the ZnO/In$_2$S$_3$ /CuSCN structure observed in the TRMC measurements (fig.8) as well as in the stationary photocurrents. For a simple interface recombination effect a saturation of the quantum efficiency with the film thickness is expected. We can only speculate about differences in the distribution of the electro static potential and band lineup. For example, the presence of the CuSCN could cause a drop in electric potential across the In$_2$S$_3$ layer. The corresponding electric field helps to drive electrons and holes to the opposite interfaces thus reducing recombination. With increasing film thickness the electric field becomes weaker and recombination losses increase. Considering the results of this work, a principle sketch of the band alignment is shown in fig.10. The long lived charge separation observed at the ZnO/In$_2$S$_3$ interface suggests that the fermi level of the In$_2$S$_3$ is close to midgap or even more closer to the valence band. It can be expected that the low conductivity of this material stems from a strong compensation of donors and acceptors which results in the observed short lifetime of the excess charge carriers.

We have shown that the annealing step of the ZnO nanorods has an impact on the efficiency of the charge separation at the ZnO/In$_2$S$_3$ interface. Reports in the literature indicate that the preparation method for In$_2$S$_3$ is even more critical. In a recent article, Savenije et al. studied the charge separation in a planar CuInS$_2$/In$_2$S$_3$/TiO$_2$ heterojunction by TRMC (19). In this structure the CuInS$_2$ is the light absorber and In$_2$S$_3$ is supposed to act as buffer layer. The preparation of In$_2$S$_3$ was similar to ours but the deposition was done at a higher temperature (400C). Interesting
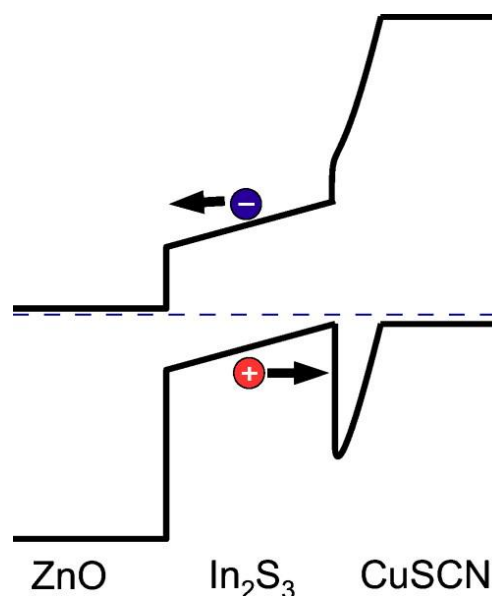

Figure 10: Illustration of a possible band alignment in the ZnO/In$_2$S$_3$/CuSCN structure compatible with the measurements.

ly, they found a rather high lifetime in In$_2$S$_3$ (58ns) but no charge separation for a In$_2$S$_3$/TiO$_2$ hetero structure. The energetic position of the bandedges in TiO$_2$ and ZnO are very similar so charge separation is expected to occur either in both or none of the two. Other reports show clearly a charge separation for In$_2$S$_3$/TiO$_2$ and In$_2$S$_3$/ZnO in electrolyte solutions, albeit with a poor IPCE of 4% (20, 21). This shows the dramatic influence of the preparation method and the need for a method that allows a quick and contactless evaluation of the photovoltaic properties of the hetero interfaces. The TRMC measurement can be a useful tool in this task. From the signal amplitude one can evaluate the charge separation efficiency related to the absorption and transport properties of the absorber.

For the further improvement of the solar cell it will be essential to improve the effective lifetime in the absorber layer to be able utilize thicker layers than the current optimum thickness of about 15nm. One crucial step will be to optimize the process of CuSCN impregnation together with the ZnO nanorod morphology. The interface between the absorber layer and the hole conducting layer plays an important role and needs to be investigated further.

5. Summary and conclusion

The ZnO-nanorod/In$_2$S$_3$/CuSCN radial hetero structure was studied by time resolved microwave conductivity. Upon excitation with 532nm light, we found a long lived (ms) charge separation at the In$_2$S$_3$/ZnO interface. In contrast, the In$_2$S$_3$/CuSCN interface did show a microwave decay time equal to the instrument response (10ns). Except for very thin (<10nm) In$_2$S$_3$ layers, the decay of the TRMC signal was found to be almost the same for the ZnO-nanorod/ In$_2$S$_3$ and ZnO-nanorod/In$_2$S$_3$/CuSCN samples.

Charge separation and Recombination in radial ZnO/In$_2$S$_3$/CuSCN heterojunction structures, J. Tornow et al..,
J. Appl. Phys. 108 (2010) 044915

8

Although there is apparently no effective charge separation at the In$_2$S$_3$/CuSCN interface, it nevertheless plays an important role for the photovoltaic efficiency of this particular hetero structure. The strong decrease of the solar cells short circuit current with increasing In$_2$S$_3$ layer thickness reported previously, was found to be the result of the charge separation efficiency depending on the thickness of the In2S3 layer in the presence of CUSCN. Although the time resolution of our experiment was not sufficient to resolve recombination processes within the absorber layer, we were still able to attribute changes in the dynamics to changes in the TRMC peak amplitude. The presence of the CuSCN hole conductor increased the initial amplitude of the TRMC signal by a factor of 8 for a 6nm thick In$_2$S$_3$ layer but the enhancement in amplitude dropped strongly for thicker films. For very thin In$_2$S$_3$ absorber layers, the recombination rate of the charge separated state in the microsecond time window was significantly enhanced compared to thicker films. Most likely, this was due to additional tunneling currents and a partly direct contact between CuSCN and ZnO. Further work needs to be done to better understand chemical and physical role of the In$_2$S$_3$/CuSCN interface. Annealing of the ZnO nanorod electrodes at 450C did increase the charge separation efficiency. The analysis of the TRMC peak amplitude as a function of the incoming light flux, optical absorption and In$_2$S$_3$ absorber thickness, showed a linear increase in amplitude at excess carrier densities below 10^{18}cm^{-3} and a sublinear dependency with an exponent of 0.6 above for the annealed ZnO samples. The 'as prepared' samples showed generally smaller amplitudes and sublinear intensity dependencies with exponents between 0.6-0.7 over the whole light intensity regime. Hence, the ZnO annealing step seems to have a strong impact on the ZnO surface that improves the charge separating properties of the In$_2$S$_3$ / ZnO interface.

Acknowledgements

References

[1] O'Regan, B.; Grätzel, M. *Nature*. **1991**, *353*, 737 -740.

[2] Yu, G.; Gao, J.; Hummelen, J. C.; Wudl, F.; Heeger, A. J. *Science*. **1995**, *270*, 1789 -1791.

[3] Tian, B.; Zheng, X.; Kempa, T. J.; Fang, Y.; Yu, N.; Yu, G.; Huang, J.; Lieber, C. M. *Nature*. **2007**, *449*, 885.

[4] Takanezawa, K.; Hirota, K.; Wei, Q.; Tajima, K.; Hashimoto, K. *Journal of Physical Chemistry C*. **2007**, *111*, 7218-7223.

[5] Zhang, Y.; Wang, L.; Mascarenhas, A. *Nano Letters*. **2007**, *7*, 1264-1269.

[6] Law, M.; Greene, L.; Johnson, J.; Saykally, R.; Yang, P. *Nature Materials*. **2005**, *4*, 455-459.

[7] Levy-Clement, C.; Tena-Zaera, R.; Ryan, M.; Katty, A.; Hodes, G. *Advanced Materials*. **2005**, *17*, 1512-1515.

[8] Peterson, R. B.; Fields, C. L.; Gregg, B. A. *Langmuir*. **2004**, *20*, 5114-5118.

[9] Belaidi, A.; Dittrich, T.; Kieven, D.; Tornow, J.; Schwarzburg, K.; Lux-Steiner, M. *physica status solidi (RRL) - Rapid Research Letters*. **2008**, *2*, 172-174.

[10] Taretto, K.; Rau, U. *Progress in Photovoltaics: Research and Applications*. **2004**, *12*, 573-591.

[11] Kieven, D.; Dittrich, T.; Belaidi, A.; Tornow, J.; Schwarzburg, K.; Allsop, N.; Lux-Steiner, M. *Applied Physics Letters*. **2008**, *92*, 153107-3.

[12] Dittrich, T.; Kieven, D.; Belaidi, A.; Rusu, M.; Tornow, J.; Schwarzburg, K.; Lux-Steiner, M. C. *J Appl Phys*. **2009**, *105*, 034509-6.

[13] Kunst, M.; Beck, G. *J. Appl. Phys*. **1986**, *60*, 3558-3566.

[14] Allsop, N.; Schönmann, A.; Belaidi, A.; Muffler, H.; Mertesacker, B.; Bohne, W.; Strub, E.; Röhrich, J.; Lux-Steiner, M.; Fischer, C. *Thin Solid Films*. **2006**, *513*, 52-56.

[15] Kunst, M.; Beck, G. *J. Appl. Phys*. **1988**, *63*, 1093-1098.

[16] Sanders, A.; Hahneiser, O.; von Aichberger, S.; Kunst, M. *Solar Energy Materials and Solar Cells*. **2001**, *65*, 119-124.

[17] Engelhardt, R.; Konenkamp, R. *J. Appl. Phys*. **2001**, *90*, 4287-4289.

[18] Tornow, J.; Schwarzburg, K. *Journal Physical Chemistry C*. **2007**, *111*, 8692-8698.

[19] Savenije, T. J.; Nanu, M.; Schoonman, J.; Goossens, A. *J Appl Phys*. **2007**, *101*, 113718-7.

[20] Sirimanne, P. M.; Yasaki, Y.; Sonoyama, N.; Sakata, T. *Materials Chemistry and Physics*. **2003**, *78*, 234-238.

[21] Yasaki, Y.; Sonoyama, N.; Sakata, T. *Journal of Electroanalytical Chemistry*. **1999**, *469*, 116-122